Design and Analysis of Double-Layered Microwave Integrated Circuits Using a Finite-Difference Time-Domain Method

Ming-Sze Tong*, Hyeong-Seok Kim† and Yinchao Chen**

Abstract - In this paper, a number of double-layered microwave integrated circuits (MIC) have been designed and analyzed based on a developed finite-difference time-domain (FDTD) solver. The solver was first validated through comparisons of the computed results with those previously published throughout the literature. Subsequently, various double-layered MIC printed on both isotropic and anisotropic substrates and superstrates, which are frequently encountered in printed circuit boards (PCB), have been designed and analyzed. It was found that in addition to protecting circuits, the added superstrate layer can increase freedoms of design and improve circuit performance, and that the FDTD is indeed a robust and versatile tool for multilayer circuit design.

Keywords: double-layered MIC, FDTD.

1. Introduction

The finite-difference time-domain (FDTD) method has been shown to be a powerful technique in solving Maxwell's equations related to boundary value problems [1-3]. The algorithm has been extensively applied to solve a broad variety of electromagnetic problems due to its great flexibility in modeling arbitrary shaped structures with complex media and broad frequency band computation without any matrix operations [4-7].

In this paper, the FDTD algorithm is applied to design and analyze various planar double-layered microstrip-line circuits. Such circuits play an important rule in applications of microwave integrated circuits (MIC), owing to their remarkable features of easy fabrication, high integration, and sound performance. They can be frequently encountered in various printed circuit boards (PCBs) for computer and communication applications, *e.g.*, in the central PCB of mobile telephone handsets or laptop computers. In this research, a FDTD computer solver has been developed for the purposes of circuit design and analysis. To validate the solver, some representative structures were first analyzed by comparison with those previously published in the literature, and a good agreement has been observed in all cases. Subsequently, different MIC were designed and analyzed, including a double-layered branch line coupler, a cascaded band stop filter, and a stepped-impedance low pass filter. It has been found that the circuit characteristics can be accurately predicted and the dimensions of designed structures can be easily tuned for improving their performance with the developed FDTD tool.

* School of Electrical and Electronics Engineering, Chung-Ang University, Seoul, Korea. (mingszetong@wm.cau.ac.kr)
† Corresponding Author: School of Electrical and Electronics Engineering, Chung-Ang University, Seoul, Korea. (kimcaf2@cau.ac.kr)
** Dept. of Electrical and Computer Engineering, University of South Carolina, Columbia, SC, USA. (chenyin@engr.sc.edu)
Received September 14, 2004 ; Accepted October 20, 2004

2. Design Procedures and FDTD Setup

In this research, a Blackman-Harris window function [8] is excited at the input port of the structures for broadband computations. All supporting substrates and superstrates used are lossless dielectric materials with μ_r=1. All conducting strips as well as the ground plate, are assumed to be perfect electric conductors (PECs) and infinitesimally thin. In most cases, a 4-layer anisotropic perfectly matched layer (APML) medium [9] is employed as the absorbing boundary condition (ABCs) for all side and top walls, while an 8-layer APML medium is adopted for the boundaries at the two ends in the direction of wave propagation. The computational stability is ensured by the Courant condition [10], and a steady state time domain response is used to extract the corresponding frequency domain characteristics.

2.1 Double-Layered Branch Line Coupler

Figs. 1a and 1b, which are similar to the one described in [11], depict geometry and dimensions of a double-layered branch line coupler, whose main transmission line has a characteristic impedance of Z_0. It is a 3dB directional coupler whose function is to equally divide the power between ports 3 and 4 from either port 1 or 2 at a particular operating frequency f_0.

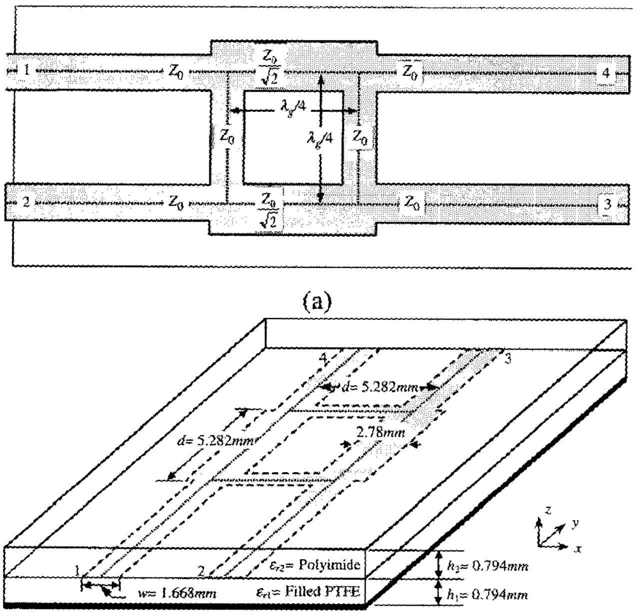

(b)

Fig. 1 Configuration of a double-layered branch line coupler (with ε_{r1}=Filled PTFE, and ε_{r2}=Polyimide). (a) Top view; (b) geometry and dimensions.

Theoretically, for the structure shown in Fig. 1a, the relationship between the operating frequency f_0 and the center-to-center distance in the middle of the square-shaped coupler, say d, can be expressed as

$$d = \frac{\lambda_g(f_0)}{4} = \frac{v_c}{4 f_0 \sqrt{\varepsilon_{eff}}} \tag{1}$$

where $\lambda_g(f_0)$ is the guided wavelength of the structure, vc denotes the speed of the wave in free-space, and εeff is the effective relative permittivity of the transmission line.

By locating the ratio of the strip width w and the height h between the strip and the ground plate, *i.e.*, w/h, the characteristic impedances, Z_0 and $Z_0/\sqrt{2}$, can be determined for the specified transmission line segments as shown in Fig. 1b. As an industrial standard, the characteristic impedance is set as $Z_0 \cong 50\Omega$.

For this coupler design, two supporting materials are used. One is the anisotropic filled PTFE cloth, with ε_{xx}=16.64, ε_{yy}=6.24, and ε_{zz}=5.56, as the substrate, while the other is the isotropic Polyimide as the superstrate, with $\varepsilon_{xx}=\varepsilon_{yy}=\varepsilon_{zz}$=3.3. Both layers are assumed to be 1/32 inch (0.794mm) in thickness. The branch-line conducting strips are sandwiched at the connecting interface of these two layers. The configuration and dimensions of this printed circuit are displayed in Fig. 1b. It has been found that $\varepsilon_{eff} \approx 4.6$ and $Z_0 \approx 50\Omega$ when w/h=1.4, while $Z_0/\sqrt{2} \cong 35.36\Omega$ when w/h=2.45. The distance d is chosen to be d=5.282mm. Hence, the corresponding operating frequency is predicted as

$$f_0 = \frac{v_c}{4d\sqrt{\varepsilon_{eff}}} = \frac{3\times10^8}{4(5.282\times10^{-3})\sqrt{4.6}} \cong 6.62GHz \tag{2}$$

A set of grids of $\Delta x=\Delta y$=0.278, and Δz=0.265mm is used. The heights of both layers are modeled at $3\Delta z$, and the center-to-center distances in the middle of the square-shaped coupler become $19\Delta x\times19\Delta y$. The total mesh dimensions are set to be $55\Delta x\times115\Delta y\times24\Delta z$ with the time step, Δt=0.524ps, and the total number of time steps, N_t=6000. Excitations are applied at port 1, which is used as the reference port for all S-parameter calculations.

2.2 Double-Layered Cascaded Band Stop Filter

A band stop filter can be realized in a cascaded manner as shown in [11]. Fig. 2 presents a double-layered configuration of such a filter, where it is assumed that all conducting strips are sandwiched by a substrate and a superstrate. By retaining the electrical length between any two adjacent stubs as $\beta l=\pi/2$ with respect to the central stop band frequency f_0,

$$l = \frac{\pi/2}{\beta} = \frac{\lambda_g(f_0)}{4} \tag{3}$$

where β and $\lambda_g(f_0)$ are, respectively, the propagation constant and the guided wavelength at f_0, and the stub length is a quarter-wavelength at the central stop band frequency.

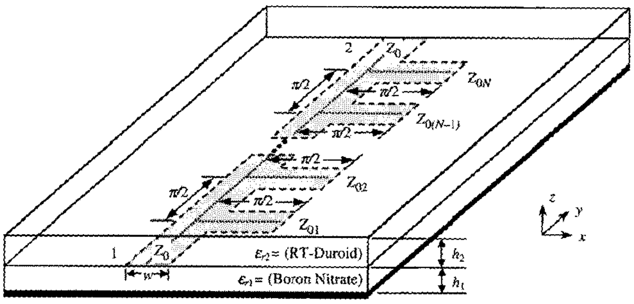

Fig. 2 Configuration of a cascaded stop band filter.

In general, each stub has its own characteristic impedance Z_{0i}, where i indicates the ith stub of the structure. Herein, for simplicity, all stubs are chosen to have the same width w as that of the main transmission line with $Z_{0i}=Z_0=50\Omega$. Again, the ratio of w/h determines the value of Z_0 for the transmission line.

In this filter design, another two sets of materials are used. An anisotropic material, the Boron Nitrate, with ε_{xx}=15.12, ε_{yy}=3.4, and ε_{zz}=5.12, is employed for the substrate, and an isotropic RT-Duroid with $\varepsilon_{xx}=\varepsilon_{yy}=\varepsilon_{zz}$=2.32, for the superstrate. Both layers have a height of

$h_1=h_2=0.64$·mm. If y is the direction of propagation, the transmission line is characterized with $\varepsilon_{eff}\approx 4.0$ and $Z_0\approx 50\Omega$ for $w/h=1.6$.

A uniform discretization grid is used with $\Delta x=\Delta y=$ 0.256mm, and $\Delta z=0.16$mm, and the main transmission line is modeled to have 4 cells on w, h_1 and h_2. The stub length is chosen to be 8 cells counted from the edge of the main transmission line. When considering the central point of the main transmission line as the starting point, the quarter-wavelength is

$$\frac{\lambda_g(f_0)}{4} = 10\times 0.256 = 2.56mm \tag{4}$$

or $\lambda_g(f_0)$=10.24mm. The corresponding central stop band frequency is

$$f_0 = \frac{v_c}{\lambda_g(f_0)\sqrt{\varepsilon_{eff}}} \approx 14.65GHz \tag{5}$$

A set of cascaded filters is considered as shown in Figs. 3a-3d up to four cascaded stub sections. The maximum mesh dimensions for the four sub-sections are $48\Delta x\times 130\Delta y\times 30\Delta z$, while Δt=0.398ps and N_t=8000.

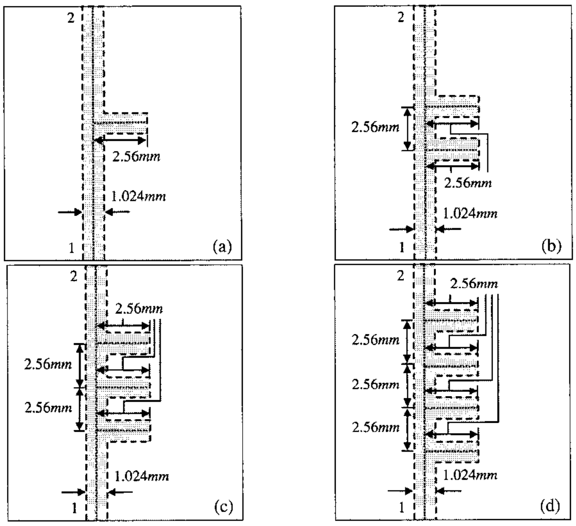

Fig. 3 Top views of cascaded band stop filters, where ε_{r1}=Boron Nitrate, ε_{r2}=RT-Duroid, and $h_1=h_2$=0.64mm. (a) One stub; (b) two stubs; (c) three stubs; (d) four stubs.

2.3 Double-Layered Stepped-Impedance Low Pass Filter

A stepped-impedance low pass filter is made of alternating sections of very high and very low characteristic impedance lines, which are specified with Z_L and Z_H, respectively. The advantage of this type of filter is low cost, and easy implementation. It should be noted that each of the alternating sections has to be short enough in order to satisfy the condition of $\beta l<\pi/4$ at the critical frequency ω_c. In such case, sections of Z_L and Z_H can be approximated as capacitive and inductive, respectively.

In this research, a double-layered stepped impedance low pass filter is designed to satisfy the following design criteria: 0.5dB equal-ripple low pass filter; critical frequency at ω_c=2.5GHz; greater than −20dB attenuation at 6.5GHz; characteristic impedances used for alternating sections are Z_L=I16Ω and Z_H=I140Ω.

In theory, the ratio of Z_H/Z_L should be as high as possible so as to obtain superior low pass property. In practice, the ratio of w/h can be tuned in order to change the values of Z_H and Z_L. For instance, the ratio can be set as w/h>>1 to reduce the value of Z_L, while w/h<<1 to increase Z_H. In addition, it is found that the smaller the substrate value ε_r, the higher the ratio of Z_H/Z_L. In particular, one way to increase the ratio of Z_H/Z_L is to use a double-layered structure, where Z_L is realized by placing the conducting strip at the central interface of the two layers, and Z_H is realized by printing the conducting strip on the top surface of the superstrate layer.

In the design, two isotropic substrates are cascaded: the substrate layer is made of Telfon with ε_{r1}=2.0, whereas the superstrate layer is made of Polystyrene with ε_{r2}=2.54 and $h_1=h_2$. Using the approach described, it has been found that $w/h\cong 13$ for Z_L, $w/h\cong 0.25$ for Z_H, and $w/h\cong 3.0$ for Z_0 of both cases in which the strip is located between the layers, or on top of the cascaded layers. For both Z_0 cases, the effective dielectric constant has been found to be $\varepsilon_{eff}\approx\varepsilon_{r1}$=2.0.

Next, the normalized frequency, $|\omega/\omega_c-1|$, is calculated to obtain the element values g_i, where i is the order of the designed filter [11]:

$$\left|\frac{\omega}{\omega_c}-1\right| = \left|\frac{6.5}{2.5}-1\right| = 1.6 \tag{6}$$

and ω is the frequency with the specified attenuation requirement.

Fig. 4 displays the relationship between the normalized frequency and the attenuation for various orders of the 0.5dB equal-ripple low pass filters. Herein it can be deduced that when the filter is in the third order, *i.e.*, n=3, the attenuation requirement would be satisfied. Table 1 gives the values of element g_i, for the first five orders of the low pass filter. The graph and the table are both reproduced from [11]-[12].

By referring to Fig. 4 and Table 1,

$$g_1=1.5963,\ g_2=1.0967,\ \text{and}\ g_3=1.5963 \tag{7}$$

These are the capacitive or inductive parameters of the stepped sections.

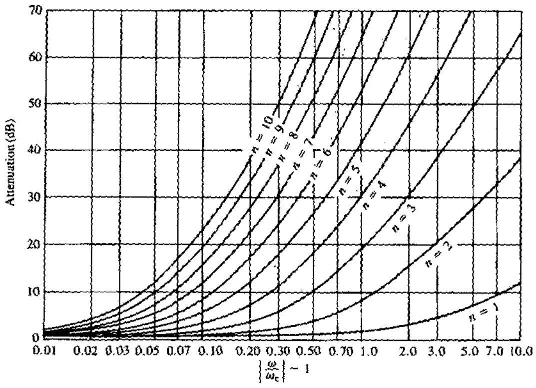

Fig. 4 Attenuation versus normalized frequency for various orders of the 0.5dB equal-ripple low pass filters.

Table 1 Element values for 0.5dB equal-ripple low pass filters (ω_c=1, n=1 to 5).

n	g_1	g_2	g_3	g_4	g_5	g_6
1	0.6986	1.0000				
2	1.4029	0.7071	1.9841			
3	1.5963	1.0967	1.5963	1.0000		
4	1.6703	1.1926	2.3661	0.8419	1.9841	
5	1.7058	1.2296	2.5408	1.2296	1.7058	1.0000

If the filter starts with a capacitive element, *i.e.*, a section with Z_L, for a third order filter, the alternating sections are in the order of Z_0–Z_L–Z_H–Z_L–Z_0. The length for each alternating section then becomes

$$l_1 = \frac{1}{\beta(\omega_c)} \cdot g_1 \cdot \frac{Z_L}{Z_0} = \frac{v_c/\left(f_c\sqrt{\varepsilon_{eff}}\right)}{2\pi} \cdot g_1 \cdot \frac{Z_L}{Z_0} = 6.90mm \tag{8a}$$

$$l_2 = \frac{1}{\beta(\omega_c)} \cdot g_2 \cdot \frac{Z_0}{Z_H} = \frac{v_c/\left(f_c\sqrt{\varepsilon_{eff}}\right)}{2\pi} \cdot g_2 \cdot \frac{Z_0}{Z_H} = 5.29mm \tag{8b}$$

$$l_3 = \frac{1}{\beta(\omega_c)} \cdot g_3 \cdot \frac{Z_L}{Z_0} = \frac{v_c/\left(f_c\sqrt{\varepsilon_{eff}}\right)}{2\pi} \cdot g_3 \cdot \frac{Z_L}{Z_0} = 6.90mm \tag{8c}$$

Note that the maximum length allowed is determined by the relation $\beta l_{max}=\pi/4$ and can be calculated as

$$l_{max} = \frac{\pi/4}{\beta(\omega_c)} = \frac{\pi}{4} \cdot \frac{v_c/\left(f_c\sqrt{\varepsilon_{eff}}\right)}{2\pi} = 10.61mm \tag{9}$$

Obviously, all sections satisfy the requirement $\beta l_i<\pi/4$.

Two different filter configurations have been constructed for this design. One is to realize Z_0 by sandwiching the conducting strip between the substrate and superstrate layers as shown in Fig. 5a, and the other is to place the strip on the top surface of the superstrate as depicted in Fig. 5b. The conducting strips of two adjacent alternating sections are connected through vertical vias. In the design, a uniform grid is used with Δx=0.20mm, Δy=0.267mm, and Δz=0.20mm. The heights of the substrate and superstrate, h_1 and h_2, are both $4\Delta z$, and the areas in the x-y plane for sections of Z_L and Z_H are $52\Delta x\times 26\Delta y$ and $2\Delta x\times 20\Delta y$, respectively. The strip width of Z_0 is modeled with $12\Delta x$ for the sandwiched case and $24\Delta x$ when the strip is on top of the two layers. The total mesh dimensions are $80\Delta x\times 165\Delta y\times 24\Delta z$, Δt=0.4148ps and N_t=5000.

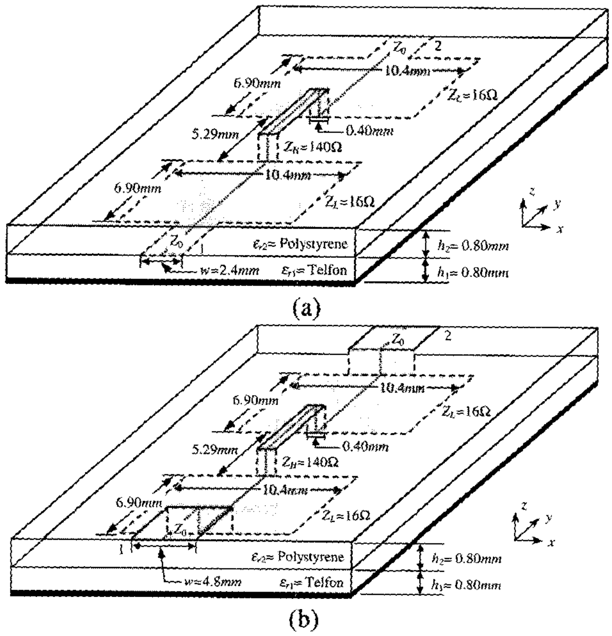

Fig. 5 Geometry and dimensions of double-layered stepped-impedance low pass filters (with ε_{r1}=Telfon, and ε_{r2}=Polystyrene). (a) Sandwiched main transmission line; (b) topped main transmission line.

3. Numerical Results

In order to verify the developed computer solver, two planar printed MIC structures that were previously studied in the literature are analyzed. The first one is a single-layered branch line coupler [13], whose configuration is depicted in Fig. 6a. The supporting substrate is the Duroid with ε_r=2.2. To test for the capability of the developed solver in handling double-layered circuits, an imaginary superstrate of ε_r=1.0 has been placed over the Duroid with the same height. The computed volume is discretized into the mesh sizes of Δx=0.406mm, Δy=0.406mm, and Δz=0.265mm, with the total mesh dimensions of $60\Delta x\times 100\Delta y\times 16\Delta z$. The height of the substrate h is $3\Delta z$, and the center-to-center distances in the middle of the square-shaped coupler become $24\Delta x\times 24\Delta y$. The first order Mur's absorbing boundary conditions (ABCs) [14] are used in truncation of every opening area. All frequency responses in terms of the S-parameters are plotted in Fig.

6b and compared with those published in the literature. It is found that the computed results are in good agreement with those given in [13]. In particular, the input power has been transmitted into ports 3 and 4 uniformly at f_0, which is approximately at 6.5GHz.

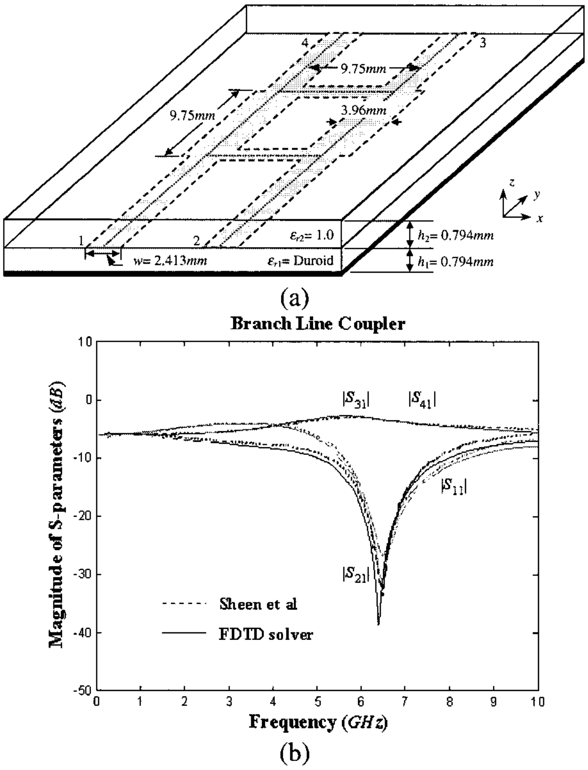

(a)

(b)

Fig. 6 (a) Geometry and dimensions of a single-layered branch line coupler covered by an imaginary superstrate; (b) magnitude of the S-parameters.

Another validation structure is a single-layered meander-line low pass filter, whose original structure was discussed by Wolff [15] as illustrated in Fig. 7a. The structure is composed of two U-shaped strips connected side-by-side with a 46Ω microstrip line. The circuit is printed on the aluminum trioxide, Al_2O_3, with ε_r=10. Again an imaginary superstrate of ε_r=1.0 has been placed to test for the capability of the solver. Herein a spatial resolution of $\Delta x=\Delta y$=0.1525, and Δz=0.15875mm, and Δt=0.296ps. The results between this method and the ones reported in [15] are given in Fig. 7b. An excellent agreement is again observed in terms of the magnitude of $S_{11}(f)$.

Next is the analysis part of the proposed designs. The first structure to be analyzed is a double-layered branch line coupler, whose geometry and dimensions are given in Figs. 1a and 1b. The plots of all frequency dependent S-parameters are provided in Fig. 8. Through Fig. 8, it is found that the computed operating frequency is approximately 6.7GHz, which is well in agreement with the expected f_0 accounted theoretically.

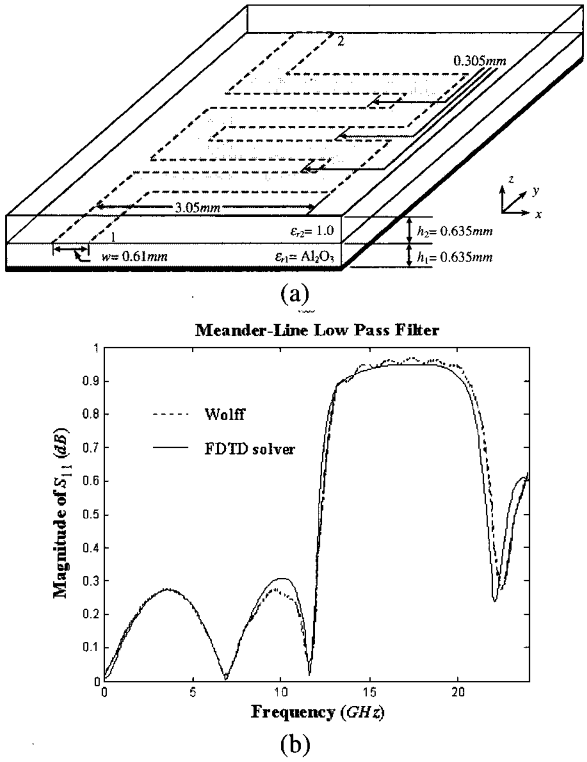

(a)

(b)

Fig. 7 (a) Geometry and dimensions of a single-layered meander-line low pass filter covered by an imaginary superstrate; (b) magnitude of $S_{11}(f)$.

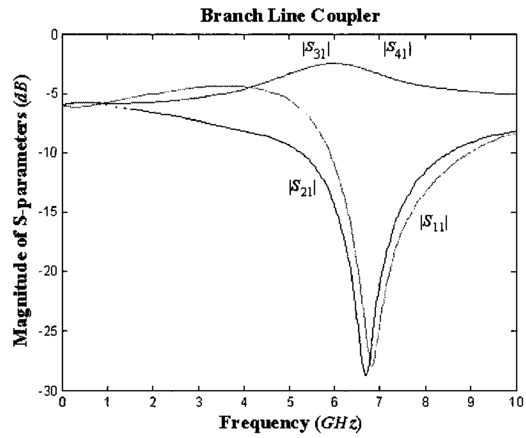

Fig. 8 Magnitude of the S-parameters for a double-layered branch line coupler.

Next, the double-layered cascaded band stop filters given in Figs. 3a-3d are analyzed, and the S-parameters for all structures are presented in Figs. 9a and 9b. When only one stub is considered, the central frequency turns out to be 15.4GHz, which is about 5.2% off the predicted one. As more stubs are connected, it is observed that both the f_0 and the depth of $S_{21}(f)$ are gradually improved, and when it comes to a 4-stub case, f_0 is found at 14.8GHz, which agrees very well to the theoretical value.

Finally, the two proposed third order stepped-impedance low pass filters as shown in Figs. 5a and 5b are designed, and Figs. 10a and 10b indicate the corresponding frequency dependent S-parameters of the designed filter. From the curve of $S_{21}(f)$, it is observed that its attenuation requirement, i.e., more than –20dB at 6.5GHz, as well as its pass band ripple, i.e., at 0.5dB variation, match the design criteria. The filter acts as a low pass structure with the critical frequency ωc, also known as the 3dB cut-off frequency, at 2.5GHz.

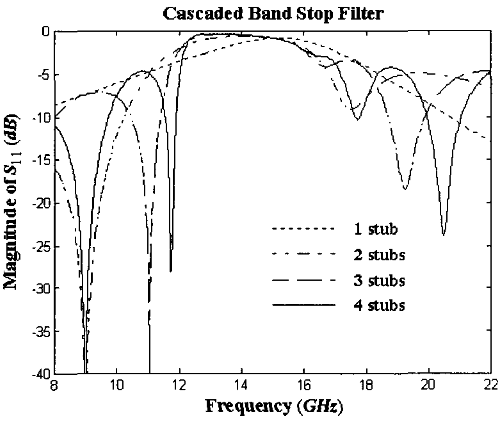

(a)

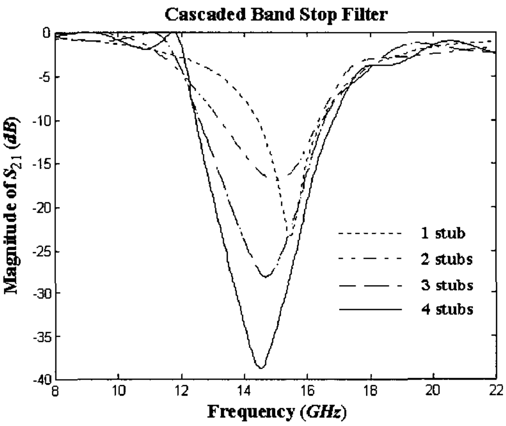

(b)

Fig. 9 (a) Geometry and dimensions of a single-layered branch line coupler covered by an imaginary superstrate; (b) magnitude of the S-parameters.

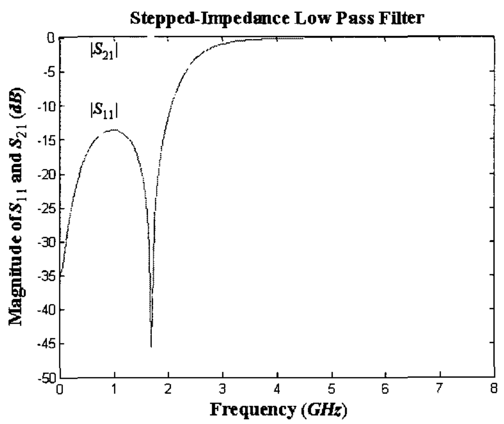

(a)

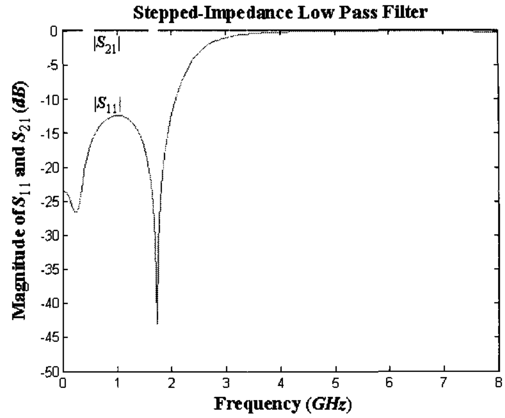

(b)

Fig. 10 Magnitude of the S-parameters for a double-layered, stepped impedance low pass filter. (a) Sandwiched main transmission line; (b) topped main transmission line.

5. Conclusion

The finite-difference time-domain (FDTD) algorithm has been successfully applied to systematically design and analyze diverse double-layered microstrip integrated circuits, which are broadly utilized in PCB applications. The validation data match excellently with those published throughout the literature, while the results in circuit design present satisfying performance when compared with the design prediction. It is observed that the FDTD is doubtlessly a robust, versatile and powerful tool for accurate prediction of characteristics of multilayered planar MICs associated with complex media.

Acknowledgement

This research was supported by Chung-Ang University Research Grants in 2004.

References

[1] K. S. Yee, "Numerical solution of initial boundary value problems involving Maxwell's equations in isotropic media," *IEEE Transactions on Antennas and Propagation*, vol. AP-14, no. 3, pp. 302-307, May 1966.

[2] A. Taflove, *Computational Electrodynamics: The Finite-Difference Time-Domain Method*, Artech House, Inc., 1995.

[3] K. S. Kunz and R. J. Luebbers, *The Finite Difference Time Domain Method for Electromagnetics*, CRC Press, Inc., 1993.

[4] D. H. Choi and W. J. R. Hoefer, "The finite difference time domain method and its application to eigenvalue problems," *IEEE Transactions on Microwave Theory and Techniques*, vol. MTT-34, no. 12, pp. 1464-1470, Dec. 1986.
[5] X. Zhang, J. Fang, K. K. Mei, and Y. Liu, "Calculations of the dispersive characteristics of microstrips by the time-domain finite difference method," *IEEE Transactions on Microwave Theory and Techniques*, vol. MTT-36, no. 2, pp. 263-267, Feb. 1988.
[6] G. Liang, Y. Liu, and K. K. Mei, "Full wave analysis of coplanar waveguide and slotline using the time-domain finite-difference method," *IEEE Transactions on Microwave Theory and Techniques*, vol. MTT-37, no. 12, pp. 1949-1957, Dec. 1989.
[7] T. Shibata, T. Hayashi and T. Kimura, "Analysis of microstrip circuits using three-dimensional full-wave electromagnetic field analysis in the time domain," *IEEE Transactions on Microwave Theory and Techniques*, vol. MTT-36, no. 6, pp. 1064-1070, June 1988.
[8] F. J. Harris, "On the use of windows for harmonic analysis with discrete Fourier transform," *Proceedings IEEE*, vol. 66, pp. 51-83, Jan. 1978.
[9] S. D. Gedney, "An anisotropic perfectly matched layer-absorbing medium for the truncation of FDTD lattices," *IEEE Transactions on Antennas and Propagation*, vol. AP-44, no. 12, pp. 1630-1639, Dec. 1996.
[10] A. Taflove and M. E. Brodwin, "Numerical solution of steady-state electromagnetic scattering problems using the time-dependent Maxwell's equations," *IEEE Transactions on Microwave Theory and Techniques*, vol. MTT-23, no. 8, pp. 623-630, Aug. 1975.
[11] D. M. Pozar, *Microwave Engineering*, Chapter 8, Section 8.5, Chapter 9, Sections 9.6 and 9.8, Addison-Wesley, USA, 1993.
[12] G. L. Matthaei, L. Young and E. M. T. Jones, *Microwave Filters, Impedance-Matching Networks, and Coupling Structures*, Artech House, Dedham, Mass., USA, 1980.
[13] D. M. Sheen, S. M. Ali, M. D. Abouzahra and J. A. Kong, "Application of the three-dimensional finite-difference time-domain method to the analysis of planar microstrip circuits," *IEEE Transactions on Microwave Theory and Techniques*, vol. MTT-38, no. 7, pp. 849-857, July 1990.
[14] G. Mur, "Absorbing boundary conditions for finite difference approximation of the time domain electromagnetic-field equations," *IEEE Transactions on Electromagnetic Compatibility*, vol. EMC-23, no. 4, pp. 377-382, Nov. 1981.
[15] I. Wolff, "Finite difference time-domain simulation of electromagnetic fields and microwave circuits," *International Journals of MIMICAE*, vol. 5, no. 3, pp. 163-182, 1992.

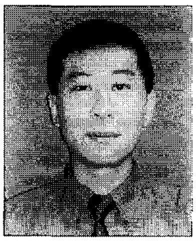

Ming-Sze Tong
He received the B.Sc. degree in Electrical Engineering from the University of Alberta, Canada, in 1991 his M.Sc. degree in Electrical Engineering from the University of Saskatchewan, Canada, in 1995, and his Ph.D. degree from the Hong Kong Polytechnic University, China, in 1999. His research areas are in computational electromagnetics and microwave engineering, mainly focused on the studies using time-domain methods. He was a Research Associate in 1999 at the Department of Electronic and Information Engineering of the Hong Kong Polytechnic University. He then worked as a Postdoctoral Fellow at the Laboratory for Electromagnetic Fields and Microwave Electronics of the Swiss Federal Institute of Technology in Zurich, Switzerland, for one year. From May 2001 to April 2002, he was a Research Fellow in the Institute of High Frequency Engineering of the Technical University of Chemnitz-Zwickau, Germany. Between August 2002 and August 2004, he was a Research Fellow in the School of Electrical and Electronic Engineering at the Nanyang Technological University, Singapore. Since September 2004, he has been a Visiting Professor in the School Electrical and Electronics Engineering at the Chung-Ang University, Korea, under support of the Institute of Information Technology Assessment Professorship Program. Dr. Tong was a recipient of the Singapore-Millennium-Foundation Postdoctoral Award in 2002-2004, a recipient of the Alexander-von-Humboldt-Foundation Fellowship in 2001-2002, and a member of the Institute of Electrical and Electronic Engineers (IEEE) Association.

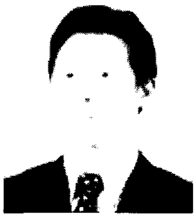

Hyeong-Seok Kim

He was born in Seoul, Korea, on October 9 1962. He received his B.S., M.S. and Ph.D. degrees in Department of the Electrical Engineering from Seoul National University, Seoul, Korea, in 1985, 1987 and 1990 respectively. From 1990 to 2002, he was with the Division of Information Technology Engineering, Soonchunhyang University, Asan, Korea. In 1997, he was a Visiting Professor of Electrical Computer Science Engineering, Rensselaer Polytechnic Institute, Troy, New York USA. In 2002, he transferred to the School of Electrical and Electronics Engineering, Chungang University, Seoul, Korea as an Associate Professor. His current research interests include numerical analysis of electromagnetic fields and waves, analysis and design of passive and active components for wireless communication, and electromagnetics education.

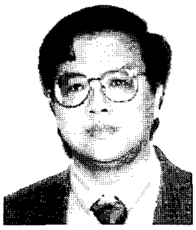

Yinchao Chen

He received his B.S. degree in space physics and his Ph. D. degree in Electrical Engineering from Wuhan University, PRC, and the University of South Carolina, USA, respectively, in 1982 and 1992. He joined the Department of Electrical Engineering, University of South Carolina, in July 2000, and currently is an Associate Professor in that Department. From 1989 to 1995, he was a Teaching and Research Assistant, Postdoctoral Fellow, Adjunct Assistant Professor, and Visiting Scholar Fellow with the University of South Carolina, South Carolina State University, and University of Illinois at Urbana-Champaign, respectively. During his earlier career in China, he was a Microwave and Antenna Engineer with the Nanjing Research Institute of Electronic Technology. He was an Assistant Professor with the Department of Electronic and Information Engineering, Hong Kong Polytechnic University, Hong Kong, during the period from 1995 to 2000. His current research interests include signal integrity for high-speed circuits, millimeter-wave integrated circuits, wireless communication applications, electronic packaging modeling for VLSI devices, microwave antenna and scattering applications. He has published over 140 international publications in refereed journals and conference symposia. He is a co-author of the book, *Multiresolution Time Domain Scheme for Electromagnetic Engineering* (John Wiley & Sons), a contributor of 6 book chapters, and a co-editor of the books *Recent Research Development of Microwave Theory and Techniques* (Research Signpost, 2002), and *Signal Integrity Engineering for Integrated Microwave and High Speed Circuits* (Research Signpost, 2005).